J Nanopart Res (2014) 16:2239
DOI 10.1007/s11051-013-2239-4

RESEARCH PAPER

Electrospinning fabrication and characterization of magnetic-upconversion fluorescent bifunctional core–shell nanofibers

Qianli Ma · Jinxian Wang · Xiangting Dong · Wensheng Yu · Guixia Liu

Received: 10 August 2013 / Accepted: 30 December 2013 / Published online: 12 January 2014

Abstract Novel magnetic-upconversion fluorescent bifunctional core–shell nanofibers have been successfully fabricated by coaxial electrospinning technology. $NaYF_4$:Yb^{3+},Er^{3+} and Fe_3O_4 nanoparticles (Nps) were incorporated into polyvinylpyrrolidone (PVP) and electrospun into core–shell nanofibers with Fe_3O_4/PVP as core and $NaYF_4$:Yb^{3+},Er^{3+}/PVP as the shell. The morphology and properties of the final products were investigated in detail by X-ray diffractometry, scanning electron microscopy, transmission electron microscopy, vibrating sample magnetometer, and fluorescence spectroscopy. The core contained magnetic Nps was ca. 100 nm in diameter, and the shell scattered with $NaYF_4$:Yb^{3+}, Er^{3+} Nps was ca. 80 nm in thickness. Fluorescence emission peaks of Er^{3+} in the [Fe_3O_4/PVP]@[$NaYF_4$:Yb^{3+},Er^{3+}/PVP] core–shell nanofibers were observed. Compared with Fe_3O_4/$NaYF_4$:Yb^{3+},Er^{3+}/PVP composite nanofibers, the luminescent intensity of the [Fe_3O_4/PVP]@[$NaYF_4$:Yb^{3+},Er^{3+}/PVP] core–shell nanofibers was much higher, because the Fe_3O_4 Nps were only distributed in the core of the core–shell nanofibers, thus the manufactured core–shell nanofibers possessed excellent magnetic properties. The new type magnetic-upconversion fluorescent bifunctional [Fe_3O_4/PVP]@[$NaYF_4$:Yb^{3+},Er^{3+}/PVP] core–shell nanofibers have many potential applications in display device, nanorobots, protein determination, and target delivery of drug owing to their excellent magnetism and fluorescence.

Keywords Electrospinning · Magnetic material · Luminescence · Core–shell nanofibers · Nanofibers

Q. Ma · J. Wang · X. Dong (✉) · W. Yu · G. Liu
Key Laboratory of Applied Chemistry and Nanotechnology at Universities of Jilin Province, Changchun University of Science and Technology, Changchun 130022, China
e-mail: dongxiangting888@163.com

Introduction

Electrospinning (Gai et al. 2013a, b; Li et al. 2013a, b, c; Ma et al. 2013c; Wang et al. 2011) is an outstanding technique to process viscous solutions or melts into continuous fibers with diameters ranging from micrometer to submicron or nanometer. This method has not only attracted extensive academic investigations but has also been applied in many areas such as filtration (Sambaer et al. 2011), optical and chemical sensors (Corres et al. 2011), biological scaffolds (Sell et al. 2011), electrode materials (Chen et al. 2011), and nanocables materials (Song et al. 2011).

Magnetic-fluorescent nanomaterials have been applied in medical diagnostics and optical imaging, etc. At present, some preparations of Fe_3O_4-RE complex core–shell structure Nps have been reported (Lu et al. 2010; Peng et al. 2011; Wang et al. 2010c;

Feng et al. 2010; Gai et al. 2010). In order to obtain new morphologies of magnetic-fluorescent nanomaterials, the fabrication of one-dimensional magnetic-fluorescent nanomaterials is an urgent subject of study. In recent years, some different types of electrospun upconversion fluorescent nanofibers (Hou et al. 2011, 2012a, b, 2013) are reported, which can be used for drug delivery, cell imaging, fluorescent lamps, color displays, etc. Some magnetic nanofibers prepared by electrospinning are also emerged in the references (Wang et al. 2010a; Meng et al. 2012). However, there are few reports in the literature about the study of the magnetic-upconversion fluorescent bifunctional nanofibers. By now, the studies of Fe_2O_3/$Eu(DBM)_3$(Bath)/polyvinyl pyrrolidone (PVP) composite nanofibers (Wang et al. 2010b) and Fe_3O_4/$Eu(BA)_3$phen/PVP composite nanofibers (Ma et al. 2012b) obtained via electrospinning are emerged in the literatures. It has been proven that the existence of Fe_3O_4 or Fe_2O_3 will greatly decrease the luminescence of rare earth compounds if Fe_3O_4 or Fe_2O_3 directly contacts with the rare earth luminescent compounds. Therefore, if a strong luminescence of magnetic-luminescent bifunctional nanofibers is to be achieved, rare earth complex must be effectively isolated from Fe_3O_4 Nps to avoid direct contact. Nanostructure of core–shell nanofibers may help to realize this academic idea. Of the core–shell nanofibers, the core is composed of template PVP containing Fe_3O_4 Nps, and the shell consists of PVP containing rare earth compounds, thus it is expected that bifunctional core–shell nanofibers with excellent magnetism and luminescence will be obtained. Moreover, the obtained magnetic-upconversion fluorescent bifunctional core–shell nanofibers have not been reported in the literature.

In this paper, we employ coaxial electrospinning technique to prepare magnetic-upconversion fluorescent bifunctional [Fe_3O_4/PVP]@[$NaYF_4$:Yb^{3+},Er^{3+}/PVP] core–shell nanofibers. Both the magnetic and fluorescent Nps are nontoxic (Sun et al. 2012). PVP is used as the fiber template and is a stable and biocompatible material (Siepmann et al. 2010). The upconversion fluorescence properties of [Fe_3O_4/PVP]@[$NaYF_4$:Yb^{3+},Er^{3+}/PVP] core–shell nanofibers are studied through comparison with $NaYF_4$:Yb^{3+},Er^{3+}/PVP nanofibers and Fe_3O_4/$NaYF_4$:Yb^{3+},Er^{3+}/PVP composite nanofibers. The magnetism properties of the core–shell nanofibers are also studied. Some new meaningful results are obtained.

Experimental sections

Chemicals

PVP K90 (Mw $\approx$ 90,000), Y_2O_3, Yb_2O_3, Er_2O_3, NaF, ethyleneglycol (EG), PVP K30 (Mw $\approx$ 30,000), $FeCl_3{\cdot}6H_2O$, $FeSO_4{\cdot}7H_2O$, NH_4NO_3, polyethyleneglycol (PEG, Mw $\approx$ 20,000), ammonia, anhydrous ethanol, $CHCl_3$, DMF, and deionized water were used. All the reagents are of analytical grade. The purity of Y_2O_3, Yb_2O_3, and Er_2O_3 are 99.99 %. Deionized water is homemade.

Preparation of Fe_3O_4 Nps

Fe_3O_4 Nps were obtained via a facile coprecipitation synthetic method, and PEG was used as the protective agents to prevent the particles from aggregation. One typical synthetic procedure was as follows: 5.4060 g of $FeCl_3{\cdot}6H_2O$, 2.7800 g of $FeSO_4{\cdot}7H_2O$, 4.0400 g of NH_4NO_3, and 1.9000 g of PEG 20000 were added into 100 ml of deionized water to form a uniform solution under vigorous stirring at 50 °C. To prevent the oxidation of Fe^{2+}, the reactive mixture was kept under argon atmosphere. After the mixture had been bubbled with argon for 30 min, 0.1 mol/L of $NH_3{\cdot}H_2O$ was added dropwise into the mixture, until the pH value was above 11. Then the system was continuously bubbled with argon for 20 min at 50 °C, and a black precipitate formed. The precipitates were collected from the solution by magnetic separation, washed with deionized water three times, and then dried in an electric vacuum oven for 12 h at 60 °C.

Synthesis of $NaYF_4$:Yb^{3+},Er^{3+} Nps

$NaYF_4$:Yb^{3+},Er^{3+} Nps were synthesized via a modified ethyleneglycol refluxing method, and PVP K30 was used as a surfactant. 0.8807 g of Y_2O_3, 0.3940 g of Yb_2O_3, and 0.0382 g of Er_2O_3 (Y:Yb:Er = 78:20:2, molar ratio) were dissolved in 50 ml of concentrated nitric acid and then crystallized by evaporation of excess nitric acid through heating process, and $Ln(NO_3)_3{\cdot}6H_2O$ (Ln = Y, Yb and Er) was acquired. $Ln(NO_3)_3$ ethylene glycol solution (solution I) was prepared by adding 50 ml of ethylene glycol into the above $Ln(NO_3)_3{\cdot}6H_2O$. 5.0388 g of NaF and 5.0000 g of PVP K30 were dissolved in a mixed solution of 30 mL of deionized water and 120 mL of ethylene

glycol (solution II) in a 250-mL three-necked flask with a backflow device. After having continuously bubbled solution II with argon for 30 min, solution I was added into solution II, and then the mixture was raised to 180 °C for 3 h. The as-prepared white precipitates were separated by a centrifuge, washed with deionized water for three times, and then dried in an electric vacuum oven for 12 h at 60 °C.

Fabrication of magnetic-upconversion fluorescent bifunctional core–shell nanofibers via electrospinning

In the preparation of inner electrospinning precursor solution, 3.0000 g of the as-prepared Fe_3O_4 Nps were dispersed ultrasonically in 100 mL of deionized water for 20 min. The suspension was heated to 80 °C under argon atmosphere with vigorous mechanical stirring for 30 min, and then 2 mL of oleic acid was slowly added. Reaction was stopped after heating and stirring the mixture for 40 min. The precipitates were collected from the solution by magnetic separation, washed with methyl alcohol for three times, and then dried in an electric vacuum oven for 6 h at 60 °C. All of the products were dispersed in 20.0000 g of $CHCl_3$ to form a stable emulsion, and then 0.5000 g of PVP K90 was slowly added into the emulsion with stirring to increase its viscosity for electrospinning process.

1.0000 g of the as-prepared $NaYF_4$:Yb^{3+},Er^{3+} Nps were dispersed into the mixture solution of 1.0000 g of PVP K90 and 6.6000 g of DMF as the shell electrospinning precursor solution. In this precursor solution, the mass ratio of $NaYF_4$:Yb^{3+},Er^{3+} Nps and PVP K90 was 1:1. Another two shell electrospinning precursor solutions with different $NaYF_4$:Yb^{3+},Er^{3+} Nps contents were also prepared to perform comparison experiments, in which 0.5000 and 0.3333 g of $NaYF_4$:Yb^{3+},Er^{3+} Nps were respectively added into the mixture solution of 1.0000 g of PVP K90 and 6.6000 g of DMF, and the mass ratios of $NaYF_4$:Yb^{3+},Er^{3+} Nps and PVP K90 were 1:2 and 1:3, respectively. A homemade coaxial dual-spinneret was used in this study. As shown in Fig. 1, the inner fluid was injected into the inner plastic syringe, while the shell fluid was loaded into the outer one. A flat iron net was used as a fiber collector and put about 14 cm away from the spinneret. A positive direct current (DC) voltage of 13 kV was applied between the spinneret and the collector to generate stable, continuous PVP-based core–shell nanofiber at ambient temperature of 22–24 °C and the relative humidity of 44–48 %.

Fabrication of Fe_3O_4/$NaYF_4$:Yb^{3+},Er^{3+}/PVP composite nanofibers and $NaYF_4$:Yb^{3+},Er^{3+}/PVP nanofibers

In order to demonstrate the structure advantages of the magnetic-upconversion fluorescent bifunctional [Fe_3O_4/PVP]@[$NaYF_4$:Yb^{3+},Er^{3+}/PVP] core–shell nanofibers, Fe_3O_4/$NaYF_4$:Yb^{3+},Er^{3+}/PVP composite nanofibers were also fabricated via traditional single-spinneret electrospinning setup as a comparison sample. The fabrication of the Fe_3O_4/$NaYF_4$:Yb^{3+},Er^{3+}/PVP composite nanofibers is a simple way of realizing the preparation of the magnetic-upconversion fluorescent bifunctional nanomaterial which mixes the Fe_3O_4 Nps, $NaYF_4$:Yb^{3+},Er^{3+} Nps, and PVP K90 together in a certain ratio as the precursor solution and electrospun into composite nanofibers. The precursor solution was prepared by mixing the inner and shell precursor solution for the fabrication of [Fe_3O_4/PVP]@[$NaYF_4$:Yb^{3+},Er^{3+}/PVP] core–shell nanofibers at the volume ratio of 1:1, and the other spinning parameters were the same as they were in the fabrication of the core–shell nanofibers.

Meanwhile, $NaYF_4$:Yb^{3+},Er^{3+}/PVP nanofibers, which have the same component as the shell of the [Fe_3O_4/PVP]@[$NaYF_4$:Yb^{3+},Er^{3+}/PVP] core–shell nanofibers, were also prepared to study the impact of magnetic core of the [Fe_3O_4/PVP]@[$NaYF_4$:Yb^{3+},Er^{3+}/PVP] core–shell nanofibers on the fluorescent property of the core–shell nanofibers. The $NaYF_4$:Yb^{3+},Er^{3+}/PVP nanofibers were electrospun using the shell precursor solution for the fabrication of [Fe_3O_4/PVP]@[$NaYF_4$:Yb^{3+},Er^{3+}/PVP] core–shell nanofibers by traditional single-spinneret electrospinning setup, and the other spinning parameters were also the same as they were in the fabrication of the core–shell nanofibers.

Characterization

The as-prepared samples were identified by an X-ray powder diffractometer (XRD, Bruker, D8 FOCUS) with Cu Kα radiation. The operation voltage and current were kept at 40 kV and 20 mA, respectively. The morphology and internal structure were observed

by a field emission scanning electron microscope (FESEM, XL-30) and a transmission electron microscope (TEM, JEM-2010), respectively. The fluorescent properties were investigated by Hitachi fluorescence spectrophotometer F-7000 with a 980-nm diode laser. Then, the magnetic performances were measured by a vibrating sample magnetometer (VSM, MPMS SQUID XL). All the measurements were performed at room temperature.

Results and discussion

XRD analyses

The phase compositions of the Fe_3O_4 Nps, $NaYF_4$:Yb^{3+},Er^{3+} Nps, and [Fe_3O_4/PVP]@[$NaYF_4$:Yb^{3+},Er^{3+}/PVP] core–shell nanofibers were characterized by means of XRD analysis, as shown in Fig. 2. The XRD patterns of the as-prepared Fe_3O_4 Nps conform to the cubic structure of Fe_3O_4 (PDF 74-0748), and no characteristic peaks are observed for other impurities such as Fe_2O_3 and FeO(OH). The XRD patterns of the $NaYF_4$:Yb^{3+},Er^{3+} Nps could be indexed to the cubic $NaYF_4$ (PDF 06-0342). The XRD analysis result of [Fe_3O_4/PVP]@[$NaYF_4$:Yb^{3+},Er^{3+}/PVP] core–shell nanofibers demonstrates that the obtained core–shell nanofibers contain both Fe_3O_4 Nps and $NaYF_4$:Yb^{3+},Er^{3+} Nps. Because the relative intensities of the XRD peaks of Fe_3O_4 Nps are much weaker than those of the $NaYF_4$:Yb^{3+},Er^{3+} Nps and Fe_3O_4 Nps are in the core of the core–shell nanofibers, it can be seen that the diffraction peaks of Fe_3O_4 are not obvious in the [Fe_3O_4/PVP]@[$NaYF_4$:Yb^{3+},Er^{3+}/PVP] core–shell nanofibers, although the content of Fe_3O_4 Nps is richer than that of $NaYF_4$:Yb^{3+},Er^{3+} Nps in core–shell nanofibers.

Morphology and structure

The morphology of the as-prepared Fe_3O_4 Nps was observed by means of SEM, as presented in Fig. 3a. The size distribution of the spherical Fe_3O_4 Nps is almost uniform, and the particle size of the Nps is 8–10 nm. The $NaYF_4$:Yb^{3+},Er^{3+} Nps were characterized by means of TEM observation, as shown in Fig. 3b. The $NaYF_4$:Yb^{3+},Er^{3+} Nps are spherical in shape and are 20–25 nm in particles size. Each $NaYF_4$:Yb^{3+},Er^{3+} nanoparticle is coated by a low-contrast shell due to the coating of the amorphous surfactant PVP K30.

The morphology and inner structure of [Fe_3O_4/PVP]@[$NaYF_4$:Yb^{3+},Er^{3+}/PVP] core–shell nanofibers were characterized by SEM and TEM observation, respectively. As seen from Fig. 4a, the surface of the [Fe_3O_4/PVP]@[$NaYF_4$:Yb^{3+},Er^{3+}/PVP] core–shell nanofibers is not smooth, and many Nps with the diameter of ca. 25 nm which are consistent with the size of $NaYF_4$:Yb^{3+},Er^{3+} Nps can be observed on the surface of the core–shell nanofibers. The diameter of the core–shell nanofibers is ca. 260 nm. Figure 4b reveals the inner structure of the [Fe_3O_4/PVP]@[$NaYF_4$:Yb^{3+},Er^{3+}/PVP] core–shell nanofibers, one can see that a large number of Nps with the diameter of ca. 10 nm is scattered throughout the core of the core–

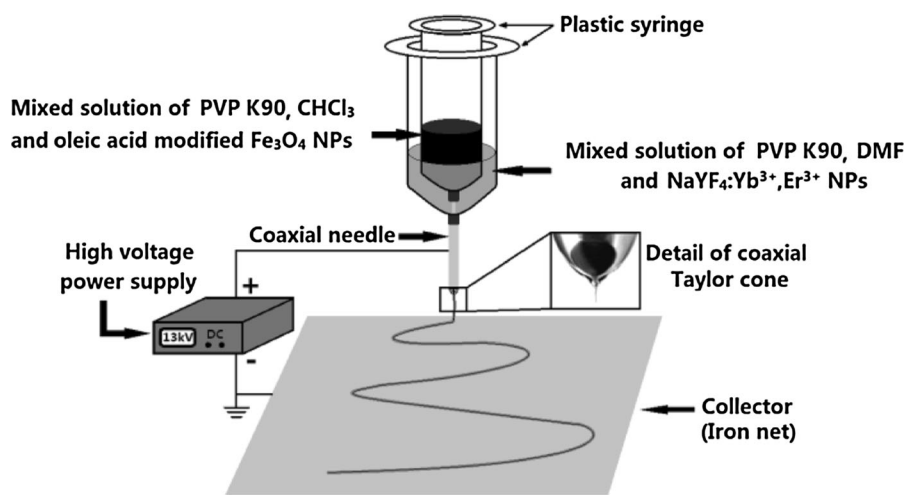

Fig. 1 Schematic diagram of the homemade coaxial electrospinning spinneret and the electrospinning setup, in which the *inset* shows the detail of core–shell Taylor cone

shell nanofibers, and the core diameter of the core–shell nanofibers is ca. 80 nm. The shell of the core–shell nanofibers is ca. 100 nm in thickness and is composed of Nps with the diameter of ca. 25 nm, and some of the nanoparticle aggregates protrude out of the surface of the core–shell nanofibers. These Nps can be identified to be $NaYF_4$:Yb^{3+},Er^{3+} Nps due to the same particle size. Through the SEM and TEM analyses in Fig. 4a,b, we can confirm that the [Fe_3O_4/PVP]@[$NaYF_4$:Yb^{3+},Er^{3+}/PVP] core–shell nanofibers were successfully prepared.

The morphology and inner structure of the Fe_3O_4/$NaYF_4$:Yb^{3+},Er^{3+}/PVP composite nanofibers were shown in Fig. 4c,d. It can be seen that the diameter of the composite nanofibers is ca. 260 nm, and Fe_3O_4 and $NaYF_4$:Yb^{3+},Er^{3+} Nps are dispersed randomly in the composite nanofibers. The surface of the composite nanofibers is more smooth than that of the [Fe_3O_4/PVP]@[$NaYF_4$:Yb^{3+},Er^{3+}/PVP] core–shell nanofibers, which may be because the $NaYF_4$:Yb^{3+},Er^{3+} Nps have larger dispersion region in the Fe_3O_4/$NaYF_4$:Yb^{3+},Er^{3+}/PVP composite nanofibers (260 nm in diameter) than in the [Fe_3O_4/PVP]@[$NaYF_4$:Yb^{3+},Er^{3+}/PVP] core–shell nanofibers (80 nm in thickness). That is, the Fe_3O_4/$NaYF_4$:Yb^{3+},Er^{3+}/PVP composite nanofibers can provide adequate space to store the $NaYF_4$:Yb^{3+},Er^{3+} nanoparticle aggregates.

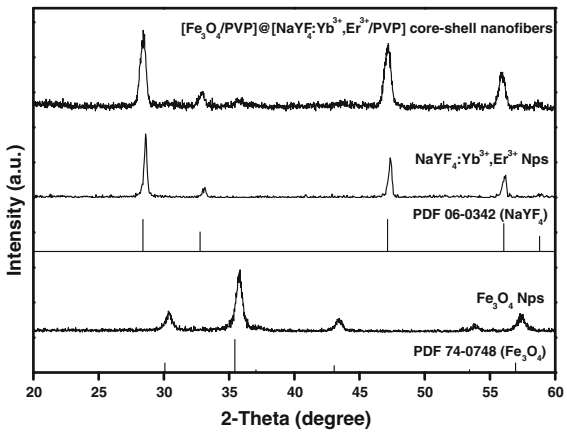

Fig. 2 XRD patterns of the Fe_3O_4 Nps, $NaYF_4$:Yb^{3+},Er^{3+} Nps, and [Fe_3O_4/PVP]@[$NaYF_4$:Yb^{3+},Er^{3+}/PVP] core–shell nanofibers

Upconversion fluorescent performance

The [Fe_3O_4/PVP]@[$NaYF_4$:Yb^{3+},Er^{3+}/PVP] core–shell nanofibers emit bright red luminescence under exciting with a 980 nm diode laser when observed by naked eye. The upconversion luminescence spectra (Fig. 5a) obtained from the core–shell nanofibers show the characteristic red and green upconverted light with red being far more intense than the green one, which means the core–shell nanofibers have good monochromaticity. The peak at 542 nm is ascribed to the transitions from the $^4S_{3/2}$ levels to the ground state ($^4I_{15/2}$), and the peak at 654 nm is corresponded to the transition from the $^4F_{9/2}$ to $^4I_{15/2}$ energy levels of the Er^{3+} doped in the $NaYF_4$:Yb^{3+},Er^{3+} nanoparticles which were introduced into the core–shell nanofibers. In the upconversion processes, the intensity of each emitting light is in proportion to the infrared excitation power: $I_{up} \alpha P^n$, where I_{up} and P^n represent the upconversion luminescence intensity and the infrared

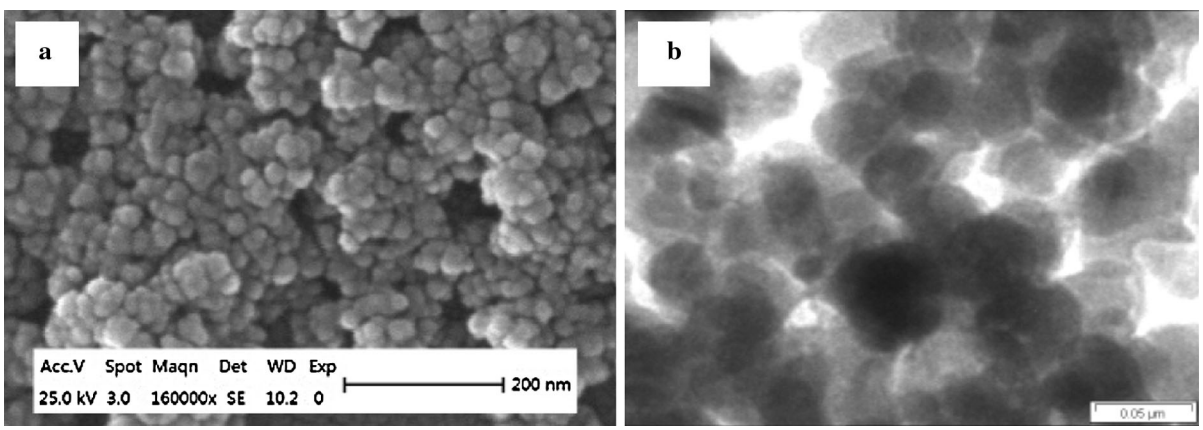

Fig. 3 SEM image of Fe_3O_4 Nps (**a**) and TEM image of $NaYF_4$:Yb^{3+},Er^{3+} Nps (**b**)

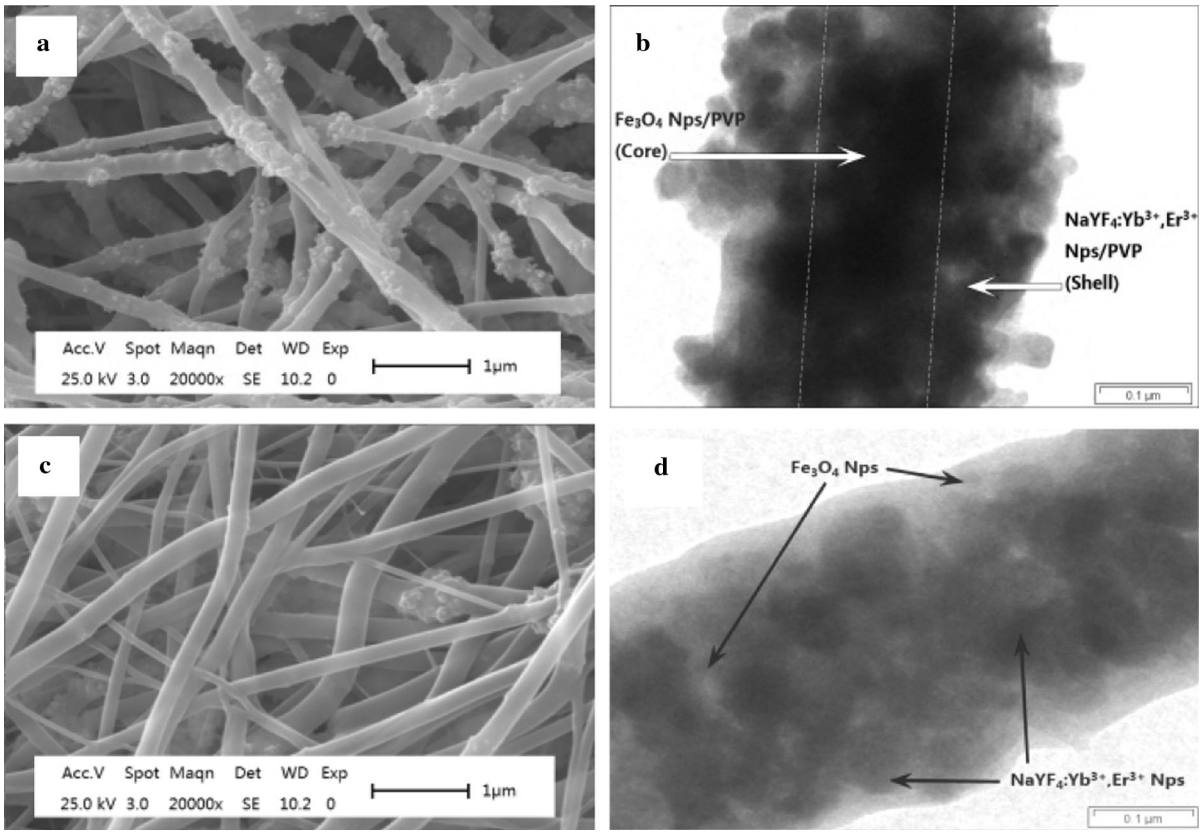

Fig. 4 SEM image (**a**) and TEM image (**b**) of [Fe_3O_4/PVP]@[$NaYF_4$:Yb^{3+},Er^{3+}/PVP] core–shell nanofibers; and SEM image (**c**) and TEM image (**d**) of Fe_3O_4/$NaYF_4$:Yb^{3+},Er^{3+}/PVP composite nanofibers

excitation intensity, respectively, and *n* (the slope) is the number of photons required to produce an upconversion photon (Yi et al. 2002). The plots of natural logarithm intensity of the upconversion emission versus natural logarithm pumped power of the core–shell nanofibers (Fig. 5b) were drawn according to the power dependence of upconversion luminescence intensity shown in Fig. 5a. The slopes are 2.220 and 2.318 for the green and red emissions, respectively. These results indicate that two photon is required to produce a visible photon in the core–shell nanofibers.

The upconversion emission intensities of the [Fe_3O_4/PVP]@[$NaYF_4$:Yb^{3+},Er^{3+}/PVP] core–shell nanofibers containing different amounts of $NaYF_4$:Yb^{3+},Er^{3+} Nps are investigated by changing the mass ratio of $NaYF_4$:Yb^{3+},Er^{3+} Nps to PVP in the preparation of the shell electrospinning precursor solution, and the results are shown in Fig. 6. It is obvious that the upconversion emission intensity is increased with the increase of the amount of $NaYF_4$:Yb^{3+},Er^{3+} Nps introduced into the core–shell nanofibers, and it is possible to tune the upconversion emission intensity of the core–shell nanofibers by introducing various amounts of $NaYF_4$:Yb^{3+},Er^{3+} Nps.

To illustrate the advantages of the core–shell nanostructure of the magnetic-upconversion fluorescent bifunctional nanofibers, the Fe_3O_4/$NaYF_4$:Yb^{3+},Er^{3+}/PVP composite nanofibers and $NaYF_4$:Yb^{3+},Er^{3+}/PVP nanofibers, as the comparative samples, were fabricated in this paper. From the comparison of upconversion emission intensities of the three samples, as indicated in Fig. 7b, it is found that the $NaYF_4$:Yb^{3+},Er^{3+}/PVP nanofibers have the highest upconversion emission intensity. The emission intensity of [Fe_3O_4/PVP]@[$NaYF_4$:Yb^{3+},Er^{3+}/PVP] core–shell nanofibers is only a little bit lower than that of the $NaYF_4$:Yb^{3+},Er^{3+}/PVP nanofibers. The Fe_3O_4/$NaYF_4$:Yb^{3+},Er^{3+}/PVP composite nanofibers obviously have the lowest emission intensity. This phenomenon may

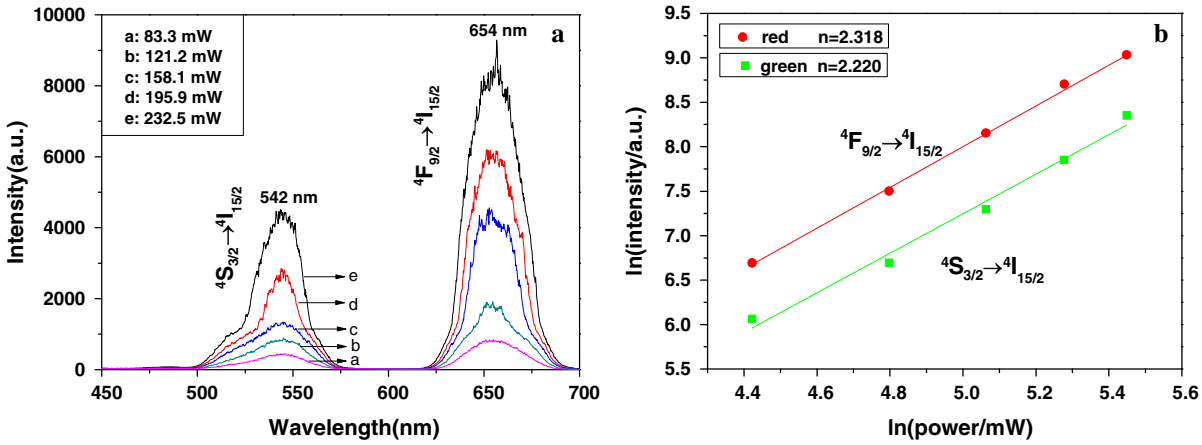

Fig. 5 Upconversion emission spectra of [Fe_3O_4/PVP]@[$NaYF_4$:Yb^{3+},Er^{3+}/PVP] core–shell nanofibers (**a**) excited by a 980-nm diode laser with different pumped powers and plots of natural logarithm intensity (**b**) of the upconversion emission versus natural logarithm pumped power of [Fe_3O_4/PVP]@[$NaYF_4$:Yb^{3+},Er^{3+}/PVP] core–shell nanofibers

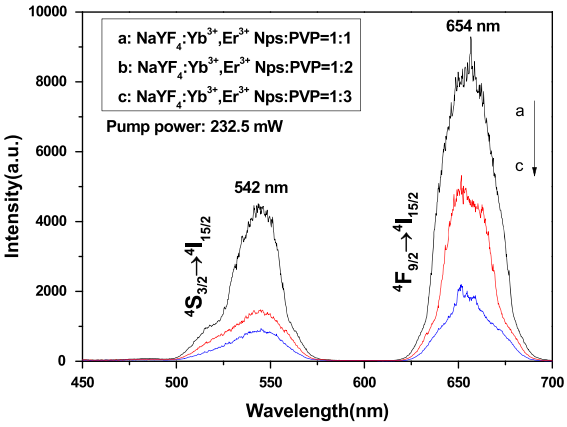

Fig. 6 Upconversion emission spectra of [Fe_3O_4/PVP]@[$NaYF_4$:Yb^{3+},Er^{3+}/PVP] core–shell nanofibers containing different mass ratios of $NaYF_4$:Yb^{3+},Er^{3+} Nps

result from the strong light absorption of Fe_3O_4 Nps which are mixed into the nanofibers (Ma et al. 2012a, 2013a; Gao et al. 2009). From the absorption spectrum of Fe_3O_4 NPs illustrated in Fig. 7a, it is seen that the Fe_3O_4 NPs can absorb light (400–1,000 nm). Thus, the exciting light and emitting light are absorbed by the Fe_3O_4 Nps and the intensities are decreased. From the contrast of the core–shell nanofibers and $NaYF_4$:Yb^{3+},Er^{3+}/PVP nanofibers, we can safely come to the conclusion that the Fe_3O_4 Nps existed in the core–shell nanofibers barely decrease the upconversion emission intensity of the core–shell nanofibers, indicating that Fe_3O_4 Nps are only in the core of the core–shell nanofibers and not in the shell of the core–shell nanofibers. As a result, the [Fe_3O_4/PVP]@[$NaYF_4$:Yb^{3+},Er^{3+}/PVP] core–shell nanofibers possess superior upconversion fluorescent properties.

A schematic diagram is proposed to explain why the existence of Fe_3O_4/PVP core barely decreases the upconversion fluorescence intensity of the [Fe_3O_4/PVP]@[$NaYF_4$:Yb^{3+},Er^{3+}/PVP] core–shell nanofibers. As seen in Fig. 8, a $NaYF_4$:Yb^{3+},Er^{3+}/PVP nanofiber is divided into three imaginary domains by dash lines. Large quantities of $NaYF_4$:Yb^{3+},Er^{3+} Nps are dispersed in the PVP K90 based nanofibers. The exciting light will be weakened due to the light absorption of the components of the fiber when it reaches the core domain, and weak emitting light is emitted. Meanwhile, the weak emitting light could barely pass through the components of the fiber to reach the external of the fiber. That is, only the $NaYF_4$:Yb^{3+},Er^{3+} Nps dispersed in the middle, and surface domains are contributed to the upconversion fluorescence intensity of the fiber. So the core domain of the fiber can be displaced by magnetic core (Fe_3O_4) and almost does not affect the fluorescence performance of the fiber.

Magnetic property

The typical hysteresis loops for Fe_3O_4 Nps, Fe_3O_4/$NaYF_4$:Yb^{3+},Er^{3+}/PVP composite nanofibers and

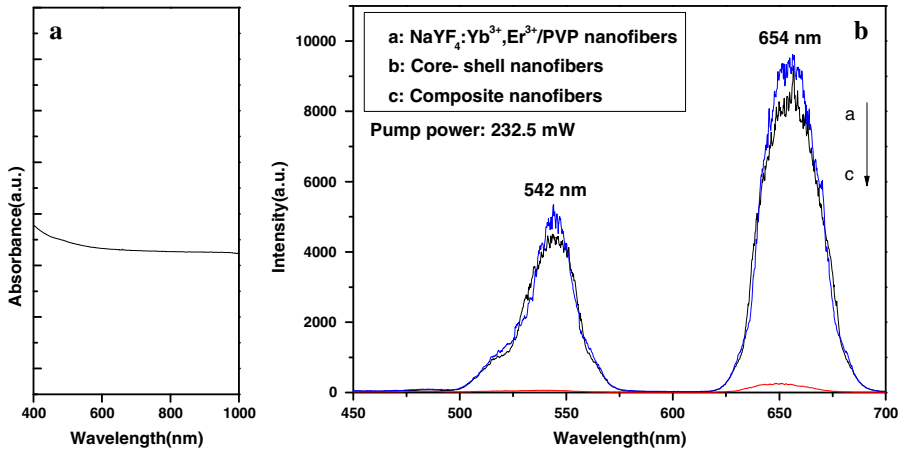

Fig. 7 UV–Vis absorbance spectrum of Fe_3O_4 NPs (**a**) and comparison among upconversion emission spectra (**b**) of [Fe_3O_4/PVP]@[$NaYF_4$:Yb^{3+},Er^{3+}/PVP] core–shell nanofibers, $NaYF_4$:Yb^{3+},Er^{3+}/PVP nanofibers and Fe_3O_4/$NaYF_4$:Yb^{3+},Er^{3+}/PVP composite nanofibers

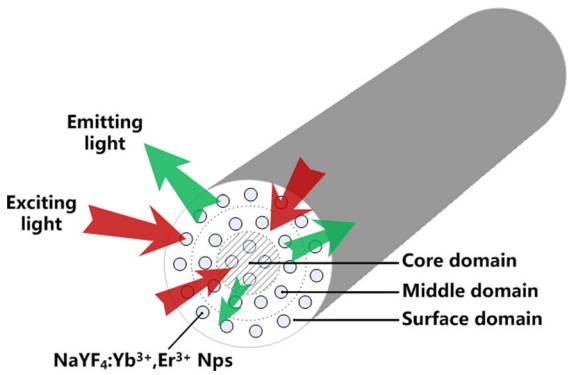

Fig. 8 Schematic diagram of the light absorption and emission of a fluorescent nanofiber

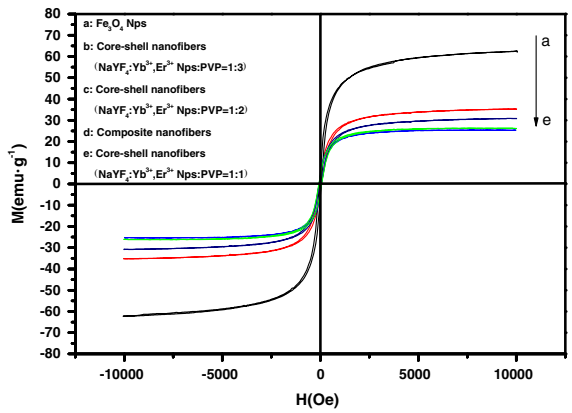

Fig. 9 Hysteresis loops of Fe_3O_4 Nps, Fe_3O_4/$NaYF_4$:Yb^{3+},Er^{3+}/PVP composite nanofibers and [Fe_3O_4/PVP]@[$NaYF_4$:Yb^{3+},Er^{3+}/PVP] core–shell nanofibers containing different mass ratios of $NaYF_4$:Yb^{3+},Er^{3+} Nps

[Fe_3O_4/PVP]@[$NaYF_4$:Yb^{3+},Er^{3+}/PVP] core–shell nanofibers containing different mass ratios of $NaYF_4$:Yb^{3+},Er^{3+} Nps are shown in Fig. 9, and the saturation magnetizations of them are listed in Table 1. It has been known that the saturation magnetization of a magnetic composite material depends on the mass percentage of the magnetic substance in the magnetic composite material (Ma et al. 2013b). From the results, the saturation magnetization of the [Fe_3O_4/PVP]@[$NaYF_4$:Yb^{3+},Er^{3+}/PVP] core–shell nanofibers is decreased with introducing more $NaYF_4$:Yb^{3+},Er^{3+} Nps into the core–shell nanofibers because the $NaYF_4$:Yb^{3+},Er^{3+} Nps are non-magnetic substance. The Fe_3O_4/$NaYF_4$:Yb^{3+},Er^{3+}/PVP composite nanofibers and [Fe_3O_4/PVP]@[$NaYF_4$:Yb^{3+},Er^{3+}/PVP] core–shell nanofibers ($NaYF_4$:PVP = 1:1) have the similar saturation magnetization which reveals that the two samples have the similar composition proportion.

By combining the analyses of magnetism and upconversion fluorescence, it is found that the [Fe_3O_4/PVP]@[$NaYF_4$:Yb^{3+},Er^{3+}/PVP] core–shell nanofibers have the similar magnetic property in comparison with the Fe_3O_4/$NaYF_4$:Yb^{3+},Er^{3+}/PVP composite nanofibers, whereas the upconversion emission intensity of the core–shell nanofibers is much higher than that of the composite nanofibers. These conclusions indicate that the core–shell nanofibers have better magnetic-upconversion fluorescent performance than the composite nanofibers.

Table 1 Saturation magnetization of Fe_3O_4 Nps, Fe_3O_4/$NaYF_4$:Yb^{3+},Er^{3+}/PVP composite nanofibers, and [Fe_3O_4/PVP]@[$NaYF_4$:Yb^{3+},Er^{3+}/PVP] core–shell nanofibers containing different mass ratios of $NaYF_4$:Yb^{3+},Er^{3+} Nps

Samples	Saturation magnetization (Ms) (emu/g)
Fe_3O_4 Nps	62.66
[Fe_3O_4/PVP]@[$NaYF_4$:Yb^{3+},Er^{3+}/PVP] core–shell nanofibers ($NaYF_4$:Yb^{3+},Er^{3+} Nps:PVP = 1:3)	35.23
[Fe_3O_4/PVP]@[$NaYF_4$:Yb^{3+},Er^{3+}/PVP] core–shell nanofibers ($NaYF_4$:Yb^{3+},Er^{3+} Nps:PVP = 1:2)	30.80
Fe_3O_4/$NaYF_4$:Yb^{3+},Er^{3+}/PVP composite	26.15
[Fe_3O_4/PVP]@[$NaYF_4$:Yb^{3+},Er^{3+}/PVP] core–shell nanofibers ($NaYF_4$:Yb^{3+},Er^{3+} Nps:PVP = 1:1)	25.43

Conclusions

In summary, uniform magnetic-upconversion fluorescent bifunctional [Fe_3O_4/PVP]@[$NaYF_4$:Yb^{3+},Er^{3+}/PVP] core–shell nanofibers were successfully synthesized by coaxial electrospinning. The diameter of the core–shell nanofibers is ca. 260 nm. The Fe_3O_4/PVP core is successfully coated with $NaYF_4$:Yb^{3+},Er^{3+}/PVP shell as a core–shell nanofiber. It's very gratifying to see that the [Fe_3O_4/PVP]@[$NaYF_4$:Yb^{3+},Er^{3+}/PVP] core–shell nanofibers possess high saturation magnetization, while the fluorescent emission intensity is barely weakened, because the Fe_3O_4 Nps are only distributed in the core of the [Fe_3O_4/PVP]@[$NaYF_4$:Yb^{3+},Er^{3+}/PVP] core–shell nanofibers. Besides, the design conception and construction technique of the core–shell nanofibers are of universal significance for the fabrication of other magnetic-luminescent core–shell nanofibers. For instance, the fluorescent color of the core–shell nanofibers can be changed by introducing other fluorescent materials into them. The fluorescent and saturation magnetic intensities of the core–shell nanofibers can also be tuned by adding different concentrations of fluorescent material and Fe_3O_4 Nps into them, respectively. The new high-performance magnetic-upconversion fluorescent core–shell nanofibers have potential applications in display device, nanorobots, protein determination, target delivery of drug, etc.

Acknowledgments This work was financially supported by the National Natural Science Foundation of China (NSFC 50972020, 51072026), Ph.D. Programs Foundation of the Ministry of Education of China (20102216110002, 20112216120003), the Science and Technology Development Planning Project of Jilin Province (Grant Nos. 20130101001JC, 20070402, 20060504), the Science and Technology Research Project of the Education Department of Jilin Province during the eleventh 5-year plan period (Under grant No. 2010JYT01), Key Research Project of Science and Technology of Ministry of Education of China (Grant No. 207026).

References

Chen SL, Hou HQ, Harnisch F, Patil SA, Carmona-Martinez AA, Agarwal S, Zhang YY, Sinha-Ray S, Yarin AL, Greiner A, Schröder U (2011) Electrospun and solution blown three-dimensional carbon fiber nonwovens for application as electrodes in microbial fuel cells. Energy Environ Sci 4:1417–1421

Corres JM, Garcia YR, Arregui FJ, Matias IR (2011) Optical fiber humidity sensors using PVdF electrospun nanowebs. IEEE Sens J 11(10):2383–2387

Feng J, Song SY, Deng RP, Fan WQ, Zhang HJ (2010) Novel multifunctional nanocomposites: magnetic mesoporous silica nanospheres covalently bonded with near-infrared luminescent lanthanide complexes. Langmuir 26:3596–3600

Gai SL, Yang PP, Li CX, Wang WX, Dai YL, Niu N, Lin J (2010) Synthesis of magnetic, up-conversion luminescent, and mesoporous core–shell-structured nanocomposites as drug carriers. Adv Funct Mater 20(7):1166–1172

Gai GQ, Wang LY, Dong XT, Xu SZ (2013a) Electrospun Fe_3O_4/PVP//$Tb(BA)_3$phen/PVP magnetic-photoluminescent bifunctional bistrand aligned composite nanofibers bundles. J Mater Sci 48:25140–25147

Gai GQ, Wang LY, Dong XT, Zheng CM, Yu WS, Wang JX, Xiao XF (2013b) Electrospinning preparation and properties of magnetic-photoluminescent bifunctional bistrand aligned composite nanofibers bundles. J Nanopart Res 15(4):1539–1547

Gao Q, Chen FH, Zhang JL, Hong GY, Ni JZ, Wei X, Wang DJ (2009) The study of novel Fe_3O_4-γ-Fe_2O_3 core/shell nanomaterials with improved properties. J Magn Magn Mater 321(8):1052–1057

Hou ZY, Li CX, Ma PA, Li GG, Cheng ZY, Peng C, Yang DM, Yang PP, Lin J (2011) Electrospinning preparation and drug-delivery properties of an up-conversion luminescent porous $NaYF_4$:Yb^{3+}, Er^{3+}-silica fiber nanocomposite. Adv Funct Mater 21(12):2356–2365

Hou ZY, Li CX, Ma PA, Cheng ZY, Li XJ, Zhang X, Dai YL, Yang DM, Lian HZ, Lin J (2012a) Up-conversion luminescent and porous $NaYF_4$:Yb^{3+}, Er^{3+}-SiO_2 nanocomposite fibers for anti-cancer drug delivery and cell imaging. Adv Funct Mater 22(13):2713–2722

Hou ZY, Li GG, Lian HZ, Lin J (2012b) One-dimensional luminescent materials derived from the electrospinning process: preparation, characteristics and application. J Mater Chem 22:5254–5276

Hou ZY, Li XJ, Li CX, Dai YL, Ma PA, Zhang X, Kang XJ, Cheng ZY, Lin J (2013) Electrospun upconversion composite fibers as dual drugs delivery system with individual release rroperties. Langmuir 29(30):9473–9482

Li D, Dong XT, Yu WS, Wang JX, Liu GX (2013a) Synthesis and upconversion luminescence properties of YF_3:Yb^{3+}/Er^{3+} hollow nanofibers derived from Y_2O_3:Yb^{3+}/Er^{3+} hollow nanofibers. J Nanopart Res 15:1704

Li D, Wang JX, Dong XT, Yu WS, Liu GX (2013b) Fabrication and luminescence properties of YF_3:Eu^{3+} hollow nanofibers via coaxial electrospinning combined with fluorination technique. J Mater Sci 48:5930–5937

Li D, Yu WS, Dong XT, Wang JX, Liu GX (2013c) Synthesis and luminescence properties of YF_3:Eu^{3+} hollow nanofibers via the combination of electrospinning with fluorination technique. J Fluor Chem 145:70–76

Lu P, Zhang JL, Liu YL, Sun DH, Liu GX, Hong GY, Ni JZ (2010) Synthesis and characteristic of the Fe_3O_4–SiO_2-$Eu(DBM)_3{\cdot}2H_2O/SiO_2$ luminomagnetic microspheres with core–shell structure. Talanta 83(1):450–457

Ma QL, Wang JX, Dong XT, Yu WS, Liu GX, Xu J (2012a) Electrospinning preparation and properties of magnetic-photoluminescent bifunctional coaxial nanofibers. J Mater Chem 22:14438–14442

Ma QL, Yu WS, Dong XT, Wang JX, Liu GX, Xu J (2012b) Electrospinning preparation and properties of Fe_3O_4/$Eu(BA)_3$phen/PVP magnetic-photoluminescent bifunctional composite nanofibers. J Nanopart Res 14(10):1203–1209

Ma QL, Wang JX, Dong XT, Yu WS, Liu GX (2013a) Electrospinning fabrication of high-performance magnetic-photoluminescent bifunctional coaxial nanocables. Chem Eng J 222(15):16–22

Ma QL, Yu WS, Dong XT, Wang JX, Liu GX, Xu J (2013b) Electrospinning fabrication and properties of Fe_3O_4/$Eu(BA)_3$phen/PMMA magnetic-photoluminescent bifunctional composite nanoribbons. Opt Mater 35:526–530

Ma WW, Dong XT, Wang JX, Yu WS, Liu GX (2013c) Electrospinning preparation of LaOBr:Tb^{3+} nanostructures and their photoluminescence properties. J Mater Sci 48(6):2557–2565

Meng FB, Zhan YQ, Lei YJ, Zhao R, Zhong JC, Liu XB (2012) Electrospun magnetic fibrillar polyarylene ether nitriles nanocomposites reinforced with Fe-phthalocyanine/Fe_3O_4 hybrid microspheres. J Appl Polym Sci 123(3):1732–1739

Peng HX, Liu GX, Dong XT, Wang JX, Xu J, Yu WS (2011) Preparation and characteristics of Fe_3O_4-YVO_4:Eu^{3+} bifunctional magnetic-luminescent nanocomposites. J Alloys Compd 509(24):6930–6934

Sambaer W, Zatloukal M, Kimmer D (2011) 3D modeling of filtration process via polyurethane nanofiber based nonwoven filters prepared by electrospinning process. Chem Eng Sci 66(4):613–623

Sell SA, Wolfe PS, Ericksen JJ, Simpson DG, Bowlin GL (2011) Incorporating platelet-rich plasma into electrospun scaffolds for tissue engineering applications. Tissue Eng Part A 17(21–22):2723–2737

Siepmann F, Eckart K, Maschke A, Kolter K, Siepmann J (2010) Modeling drug release from PVAc/PVP matrix tablets. J Control Release 141:216–222

Song J, Chen ML, Olesen MB, Wang CX, Havelund R, Li Q, Xie EQ, Yang R, Bøggild P, Wang C, Besenbacher F, Dong MD (2011) Direct electrospinning of Ag/polyvinylpyrrolidone nanocables. Nanoscale 3:4966–4971

Sun ZW, Tong LZ, Liu DM, Shi JH, Yang H (2012) Preparation and properties of multifunctional Fe_3O_4–YVO_4:Eu^{3+} or Dy^{3+} core–shell nanocomposites as drug carriers. J Mater Chem 22:6280–6284

Wang B, Sun Y, Wang HP (2010a) Preparation and properties of electrospun PAN/Fe_3O_4 magnetic nanofibers. J Appl Polym Sci 115(3):1781–1786

Wang HG, Li YX, Sun L, Li YC, Wang W, Wang S, Xu SF, Yang QB (2010b) Electrospun novel bifunctional magnetic-photoluminescent nanofibers based on Fe_2O_3 nanoparticles and europium complex. J Colloid Interf Sci 350:396–401

Wang W, Zou M, Chen KZ (2010c) Novel Fe_3O_4-YPO_4:Re (Re = Tb, Eu) multifunctional magnetic-fluorescent hybrid spheres for biomedical applications. Chem Commun 46(28):5100–5102

Wang JX, Dong XT, Cui QZ, Liu GX, Yu WS (2011) Preparation and characterization of polycrystalline $La_2Zr_2O_7$ ultrafine fibres via electrospinning. J Nanosci Nanotechnol 11:2514–2519

Yi GS, Sun BQ, Yang FZ, Chen DP, Zhou YX, Cheng J (2002) Synthesis and characterization of high-efficiency nanocrystal up-conversion phosphors: ytterbium and drbium codoped lanthanum molybdate. Chem Mater 14:2910–2914